

Supporting Information

Rapid, Large-Area Synthesis of Hierarchical Nanoporous Silica Hybrid Films on Flexible Substrates

Dong-Po Song, Aditi Naik, Shengkai Li, Alexander Ribbe, and James J. Watkins*

Experimental Section

General methods. ^1H NMR spectroscopy was recorded in CDCl_3 using a Bruker Avance DPX 300 NMR Spectrometer. Gel permeation chromatography (GPC) of the bottle brush copolymers was carried out in THF on two PLgel 10 μm mixed-B LS columns (Polymer Laboratories) connected in series with a DAWN EOS multi-angle laser light scattering (MALLS) detector and a RI detector. No calibration standards were used for the bottle brush copolymers, and dn/dc values were obtained for each injection by assuming 100% mass elution from the columns. GPC of macromonomers and polymer ligands was carried out using a Polymer Laboratories PL-GPC50 instrument with two 5 μm mixed-D columns, a 5 μm guard column, and a RI detector (HP1047A). THF was used as the eluent at a flow rate of 1.0 mL/min. Polystyrene standards were used for the calibration. Adsorption spectra were performed on a PerkinElmer LAMBDA 1050 UV/Vis/NIR spectrometer, equipped with a 150 mm integrating sphere diffuse reflectance accessory. Fourier-transform infrared spectroscopy (FTIR) measurements were carried out on a PerkinElmer FTIR spectrometer equipped with a universal ATR sampling accessory. Field emission scanning electron microscopy (FESEM) measurements were carried out on a FEI Magellan 400 FESEM. Platinum sputtering was performed on the samples for cross-sectional SEM. Transmission electron microscopy (TEM) measurements were conducted with a JEOL 2000FX TEM operated at an accelerating voltage of 200 kV. Thin sections of approximately 50 nm in thickness for microscopy were prepared using a Leica Ultracut UCT microtome equipped with a Leica EM FCS cryogenic sample

chamber operated at $-110\text{ }^{\circ}\text{C}$. *Scanning Transmission Electron Microscopy (STEM)* in *High Angle Annular Dark Field imaging mode* and *energy dispersive X-ray spectrometry (EDS)* were carried out using a JEOL JEM-2200FS at 200kV acceleration voltage and a probe size of 1.5nm. *X-ray photoelectron spectroscopy (XPS)* was performed on a Quantum 2000 Scanning ESCA Microprobe (Physical Electronics USA) using a monochromatic Al $K\alpha$ X-ray source (1486.6 eV). Typical X-ray settings used were 48 W, with 200 μm beam size, and the take off angle is 45° . XPS raw data was analyzed using Multipak, version 9.0 (Physical Electronics USA). *Small-angle X-ray scattering (SAXS)* measurements were performed with a Ganesha SAXS-LAB using 0.154 nm (Cu K radiation), sample-to-detector distance was 1,491 mm, and X-ray beam area was 0.04 mm^2 .

Sample preparation. PS-*b*-PEO brush BCP (50 mg), gold NPs (70 mg) and a commercial octamaleamic acid POSS (97 mg) were simply mixed in dimethylformamide (1.5 mL) followed by heating at $60\text{ }^{\circ}\text{C}$ for 5 minutes and vigorous stirring for 15 minutes affording a clear solution. The resulting solution was cast through $0.45\text{ }\mu\text{m}$ PTFE filters onto horizontal PET followed by drawdown rod coating. The thickness of the film can be controlled by changing the gap size of the rod. In our case, a rod with a gap size of 30 micrometer was used for the preparation of the coating resulting in a dried film with an average thickness of approximately 920 nm. The dried film was further heated to $120\text{ }^{\circ}\text{C}$ for about 20 hours in vacuum to enable NP ripening and initiate POSS crosslinking.

The photothermal processing was carried out on a Novacentrix Pulseforge 1300 photonic curing system. The light intensity was tunable via changing applied voltage and/or pulse duration time. For the optimized experimental conditions, the duration time was fixed at 0.3 millisecond and the light intensity was tuned simply by changing the applied voltage in the range from 475 to 485 V. Lower energy lead to large amounts of organic residue in the

product, while a higher energy could break the film on PET. This process includes 3 repeats of a same light pulse with a time interval of 1 second.

For the preparation of a control sample without gold nanoparticles, PS-*b*-PEO brush BCP (50 mg) and the octamaleamic acid POSS (97 mg) were simply mixed in dimethylformamide (1.0 mL) followed by vigorous stirring for 15 minutes affording a clear solution. Films were subsequently prepared using the same procedure as described for the BCP samples. Photothermal treatments were carried out using the sample experimental conditions as that used for the BCP samples. For the preparation of control samples using PEO as the template, PEO (2 kg/mol, 50 mg), gold NPs (70 mg) and the octamaleamic acid POSS (97 mg) were simply mixed in dimethylformamide (1.0 mL) followed by vigorous stirring for 15 minutes affording a clear solution. Films were subsequently prepared using the same procedure as described for the BCP samples. For the optimized experimental conditions, the duration time was fixed at 0.3 millisecond and the light intensity was tuned simply by changing the applied voltage in the range from 395 to 410 V.

Table S1. Atomic ratios of representative samples prepared using different pulse energies based on XPS analysis.

Sample	Voltage (V)	Pulse energy (mJ/cm ²)	Si2p (%)	C1s (%)	O1s (%)	Au4f (%)
control	0	0	2.50	80.4	15.6	1.5
1	475	1785	14.4	41.0	38.3	6.3
2	480	1837	16.1	39.5	37.6	6.8
3	485	1891	16.8	41.7	35.6	5.9

Supplementary Figures

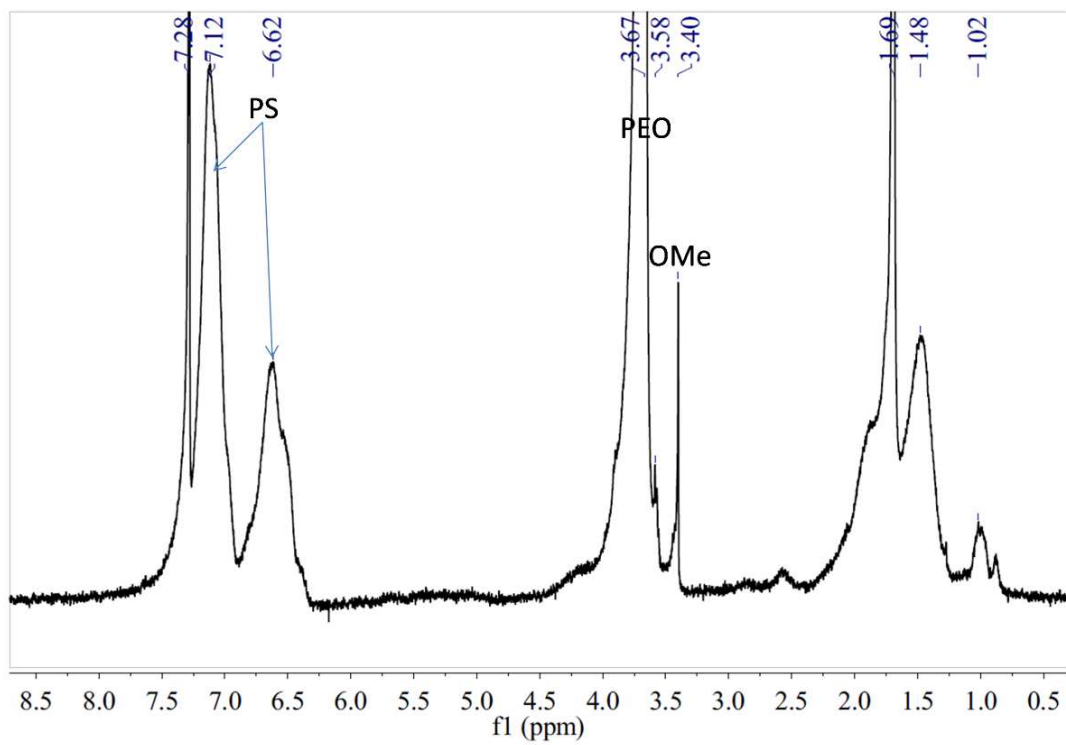


Figure S1 ^1H NMR spectrum of a PS-*b*-PEO brush BCP used in this work.

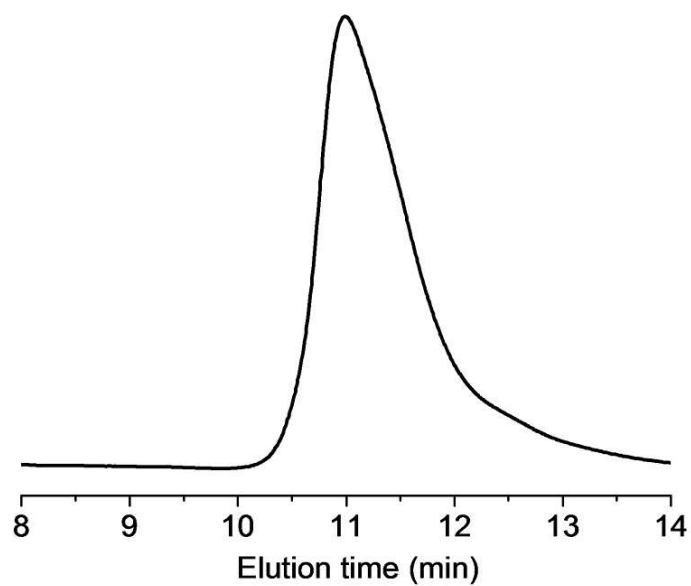


Figure S2 GPC RI trace of the PS-*b*-PEO brush BCP used in this work measured by GPC-MALLS using tetrahydrofuran as the eluent.

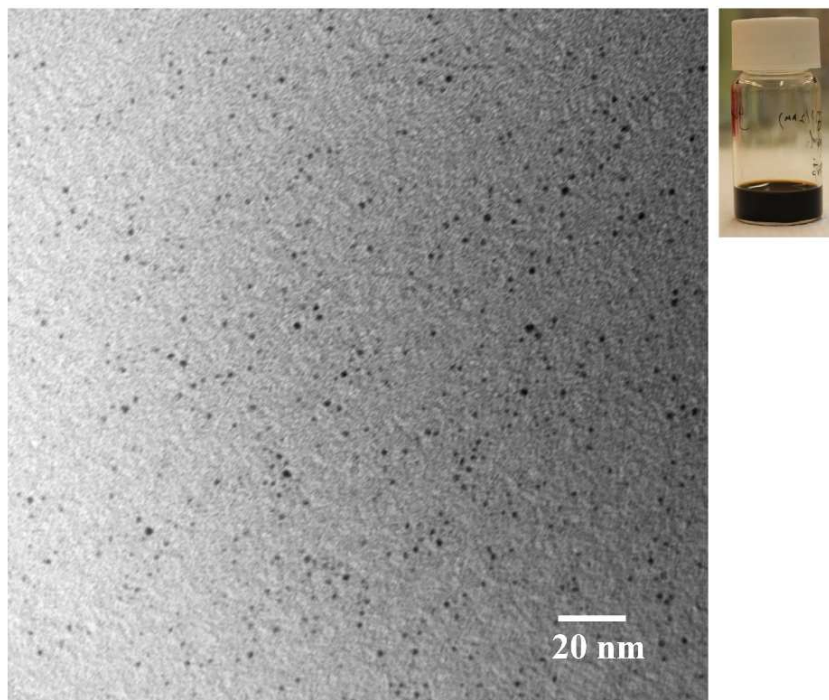


Figure S3 TEM micrograph of gold NPs used in this work. The average core diameter is approximately 2 nm.

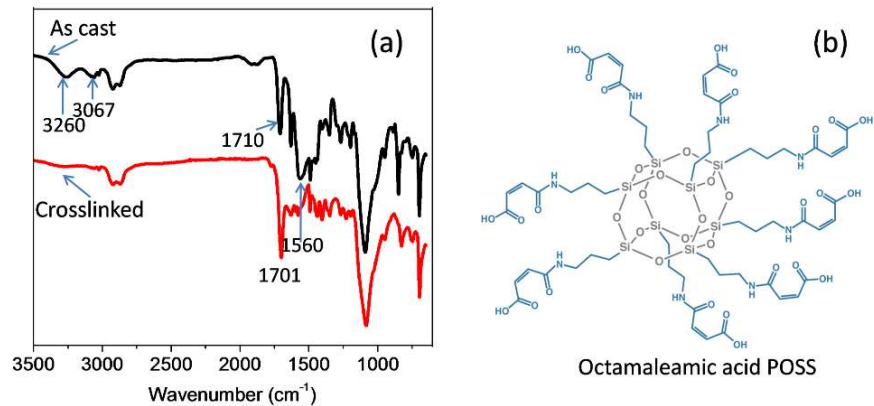


Figure S4 (a) FTIR spectra of the nanocomposites before (black) and after (red) POSS crosslinking. The crosslinking of POSS cages was achieved *via* imide formation between carboxylic acid and secondary amine groups on POSS after heating up to 120 °C. This was confirmed by the disappearance of the IR signals at 3260, 3067, and 1560 cm^{-1} , which can be ascribed to N-H stretch, O-H stretch, and N-H bend, respectively. In addition, the IR signal of C=O bond shifts from 1710 to 1701 cm^{-1} after crosslinking, which might be linked to a change in the response of carbonyl group upon reaction of carboxylic acid groups. (b) Chemical structure of the POSS used in this work.

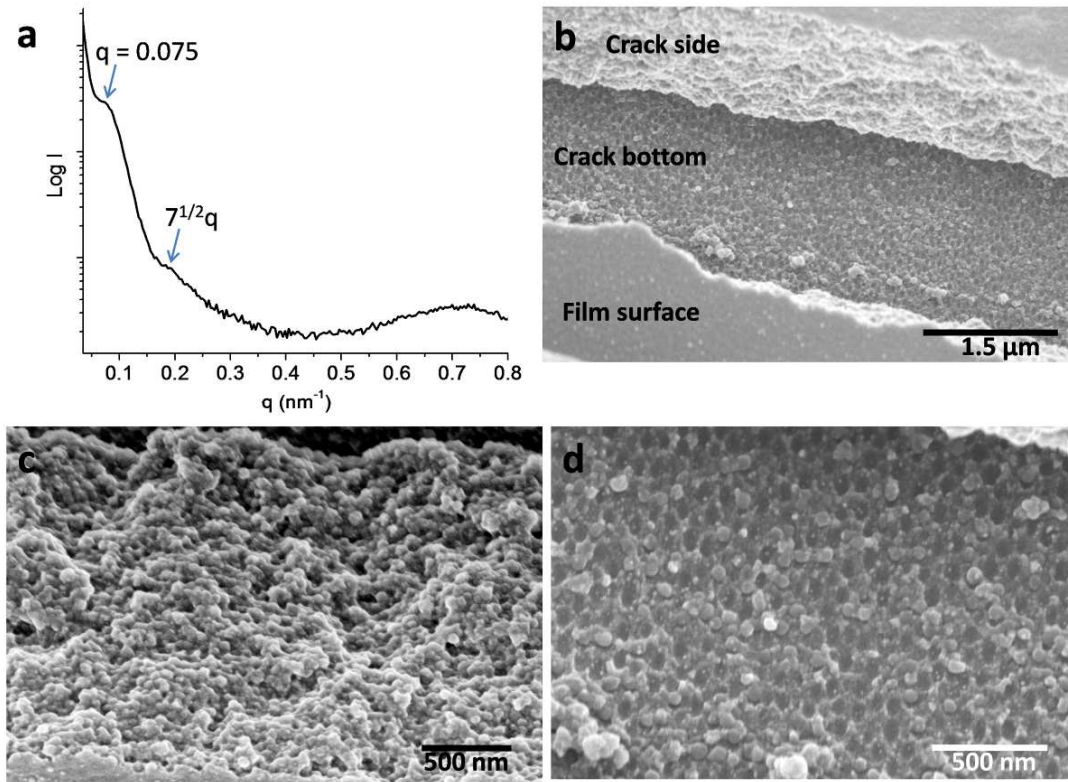


Figure S5 (a) SAXS profile of the BCP nanocomposites after evaporation from a DMF solution. An evident primary order peak as well as a weak higher scattering peak at $7^{1/2}q$ can be identified in SAXS, indicating probable formation of a spherical morphology. The domain spacing is approximately 84 nm as calculated using q of the primary order peak (d-spacing = $2\pi/q$). (b,c,d) SEM micrographs of the sample annealed at 120 °C for 20 h showing (b) a small cracking area of the film, (c) crack side viewing at a tilted angle, and (d) the bottom of the crack. Sphere-like features can be clearly seen from both side and bottom of the crack consistent with SAXS and TEM results (Figure 1b).

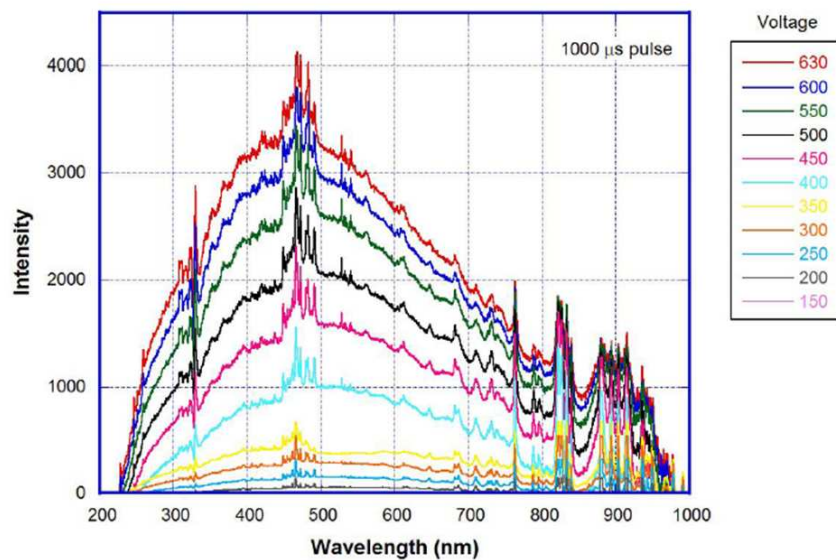


Figure S6 Emission spectra of the xenon flash lamp installed on the Pulseforge photothermal processing system at different voltages.

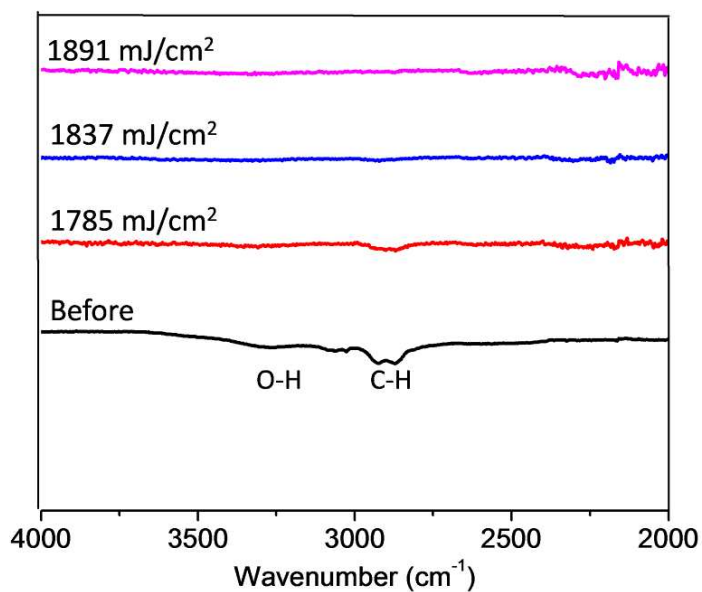


Figure S7 FTIR spectra of the BCP films before and after photothermal treatments under different light pulse energies.

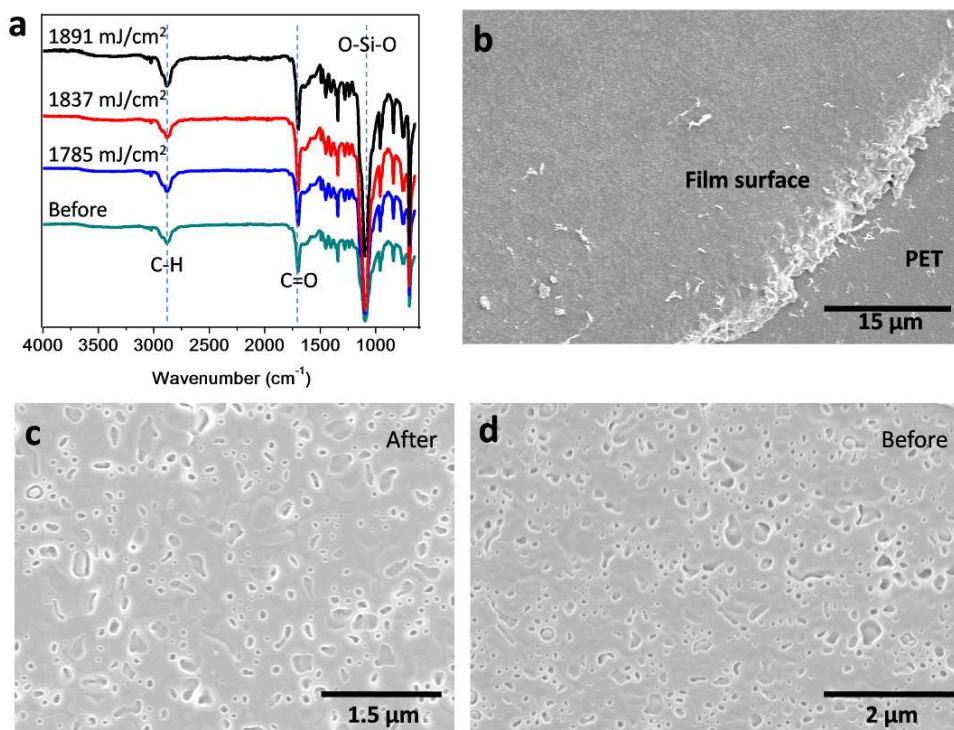


Figure S8 (a) FTIR spectra of control samples containing only the BCP and crosslinked POSS before and after photothermal treatments under different light pulse energies. The experimental conditions are identical to those used for the preparation of samples 1-3. No evident changes can be identified in FTIR before and after photothermal treatments, suggesting that the gold NPs enables the conversion of light energy to heat for the creation of nanoporous structures. (b,c) SEM micrographs of the sample prepared using light pulses of 1891 mJ/cm² showing (b) a large area of the film on PET substrate and (c) the surface area. (d) SEM micrograph showing the surface area of the film before photothermal treatment. No evident nanoporous structures can be verified in the sample in the absence of gold after the photothermal treatment.

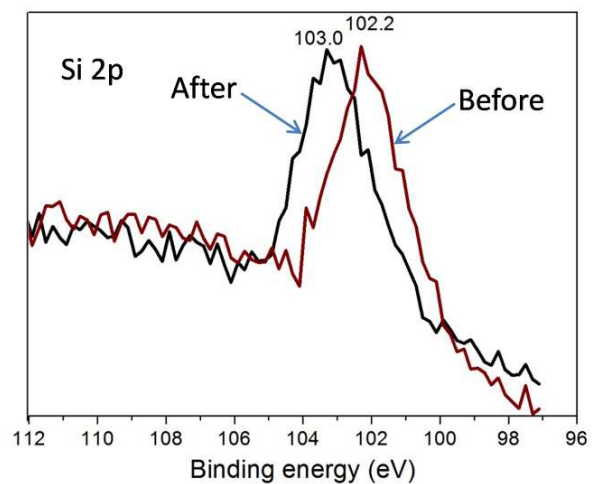


Figure S9 XPS spectra of the BCP films before (control sample) and after (sample 3) photothermal treatment showing a peak shift of silicon due to the oxidation of POSS cages.

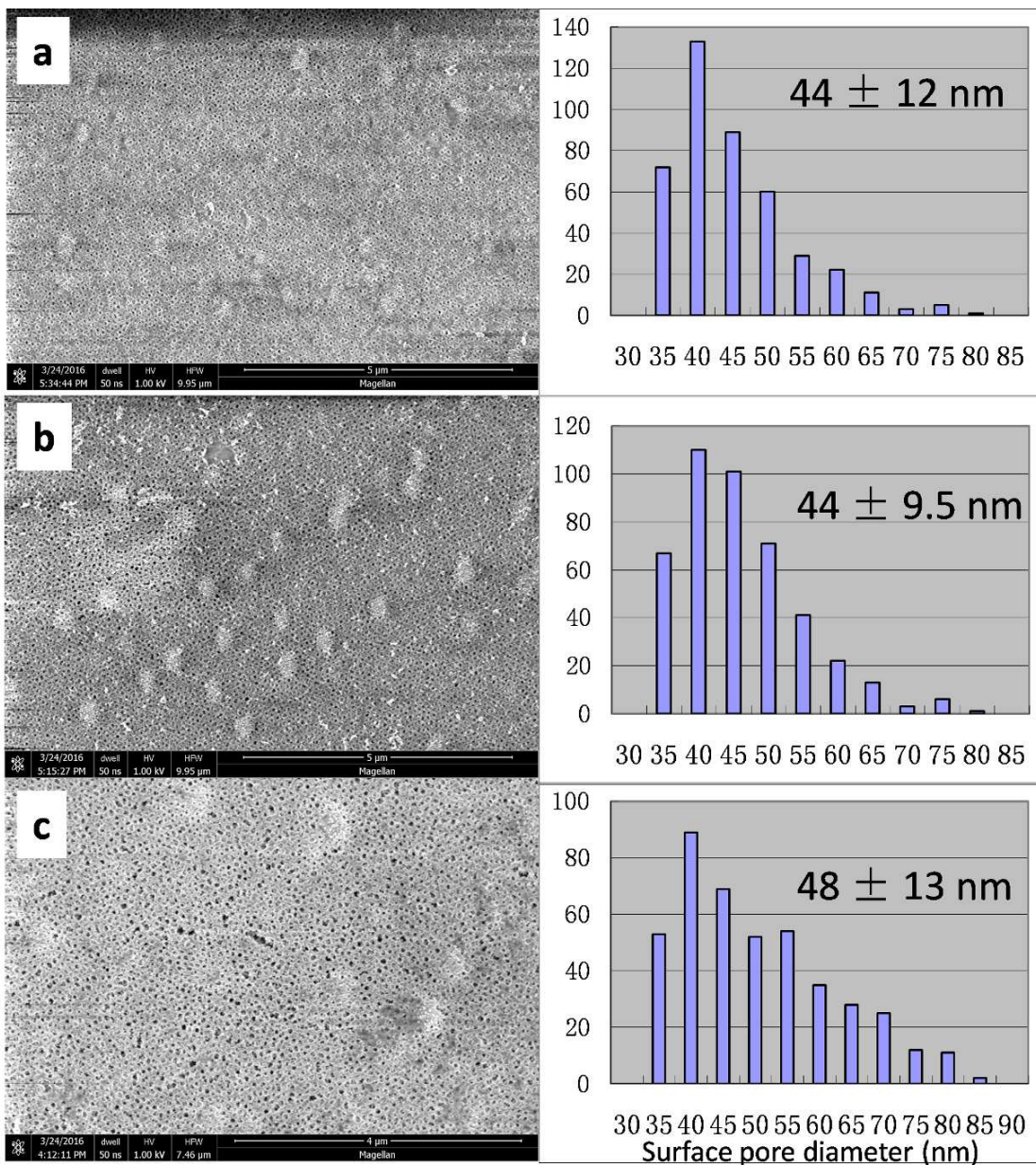


Figure S10 FESEM images of samples 1-3 prepared using different pulse energies: (a) Sample 1 (1785 mJ/cm²); (b) Sample 2 (1837 mJ/cm²); (c) Sample 3 (1891 mJ/cm²). The pore size distribution is based on image analysis of more than 400 pores using ImageJ.

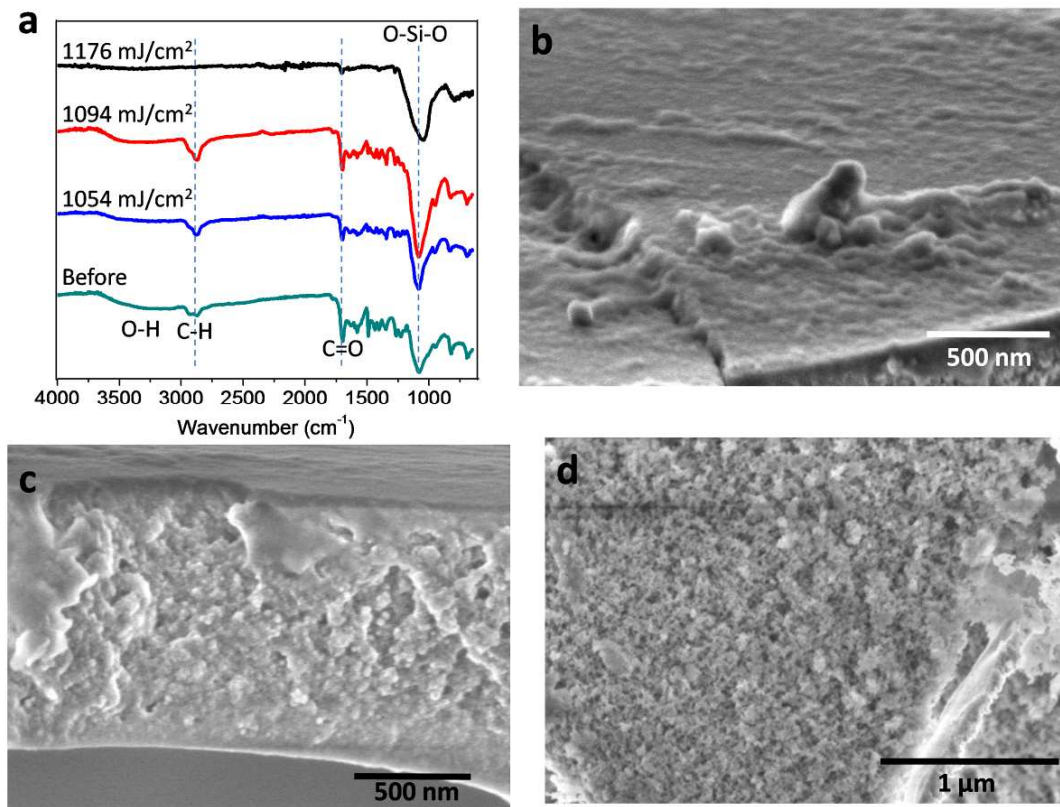


Figure S11 (a) FTIR spectra of control samples containing PEO, gold NPs, and crosslinked POSS before and after photothermal treatments under different light pulse energies. The organic components in the film can be efficiently removed at an increased light energy of 1176 mJ/cm^2 . The shift of the O-Si-O absorption peak to smaller wavenumbers indicate the oxidization of POSS to silica, which is similar to the samples prepared using the brush BCP as template (see Figure 2a). (b,c,d) SEM micrographs of the sample prepared using light pulses of 1176 mJ/cm^2 showing (b) the surface area, (c) the cross-section and (d) the surface area of a broken piece of the film. No porous structures can be seen on the film surface, while random porous structures were verified in both cross-section and broken surface regions.

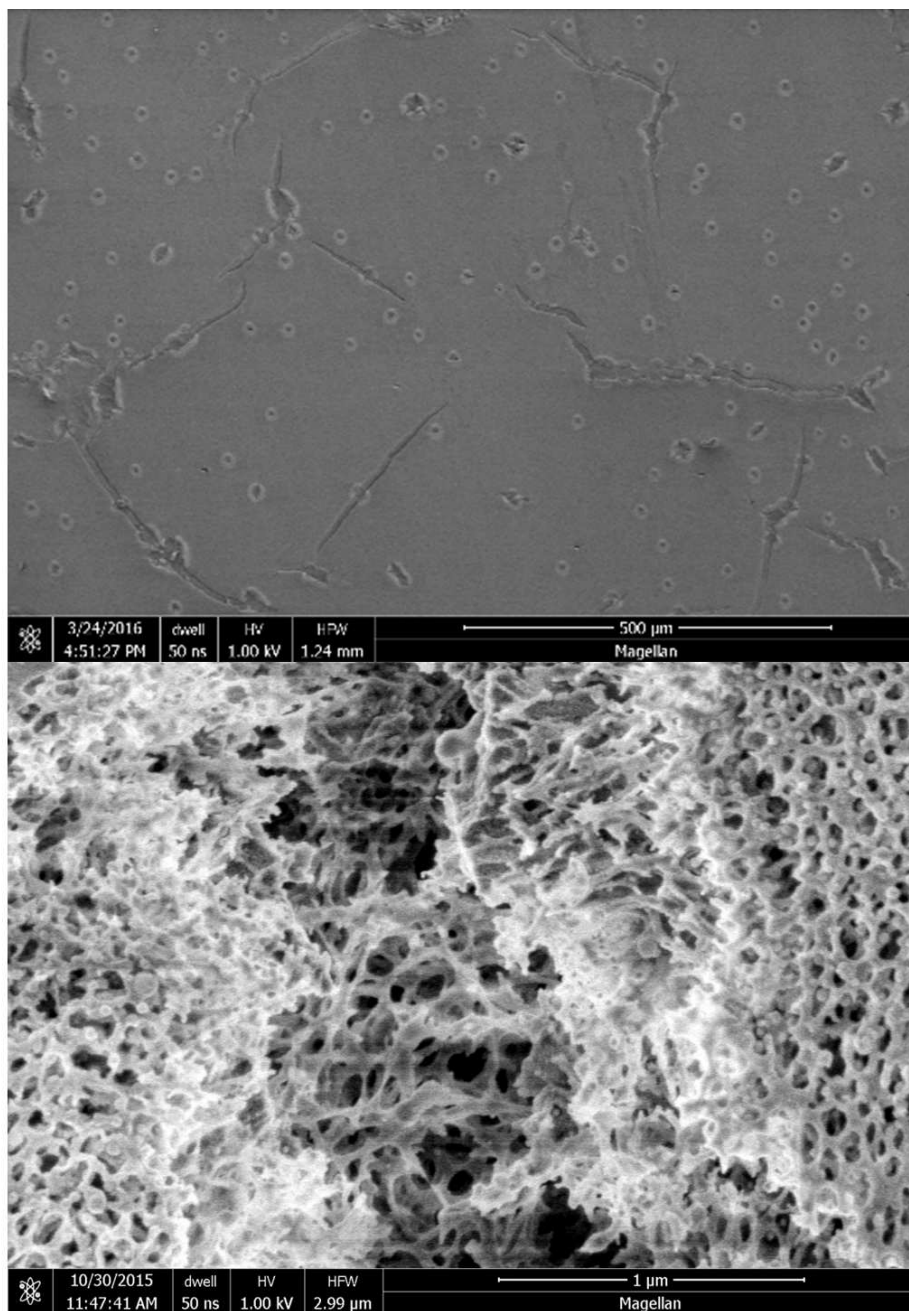


Figure S12 FESEM micrographs of the surface of sample 3 showing a foam-like structure in the small cracking area where gases were released during the photothermal processing.

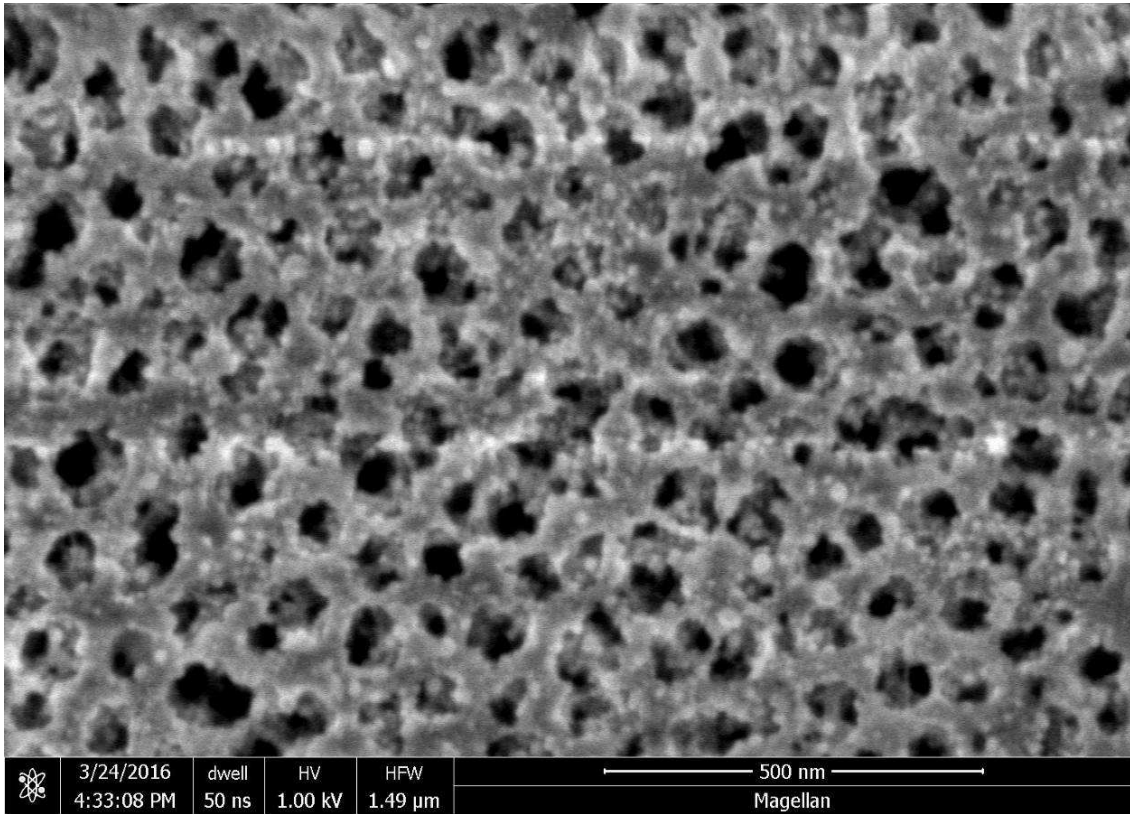


Figure S13 FESEM micrograph of sample 3 showing the opening of the surface pores to the pores underneath.